Proc. Natl. Acad. Sci. USA
Vol. 96, pp. 2794–2799, March 1999
Cell Biology

The Opitz syndrome gene product, MID1, associates with microtubules

SUSANN SCHWEIGER*†, JOHN FOERSTER‡, TANJA LEHMANN*, VANESSA SUCKOW*, YVES A. MULLER§, GERALD WALTER*, THERESA DAVIES¶, HELEN PORTER‖, HANS VAN BOKHOVEN**, PETER W. LUNT††, PETER TRAUB‡‡, AND HANS-HILGER ROPERS*,**

*Max Planck Institute for Molecular Genetics, 14195 Berlin, Germany; ‡Research Institute for Molecular Pharmacology, 12207 Berlin, Germany; §Department of Crystallography, Max Delbrück Center, 13125 Berlin-Buch, Germany; ¶Regional Cytogenetics Center, Southmead Hospital, Bristol BS2 8BJ, United Kingdom; ‖Department of Pediatric Pathology, University of Bristol BS2 8BJ, Bristol, United Kingdom; **Department of Human Genetics, University Hospital, 6500 HB Nijmegen, The Netherlands; ††Clinical Genetics Unit, Institute of Child Health, Bristol Childrens Hospital, Bristol BS2 8BJ, United Kingdom; and ‡‡Max-Planck Institute for Cell Biology, 68522 Ladenburg, Germany

Edited by Lewis G. Tilney, University of Pennsylvania, Philadelphia, PA, and approved December 21, 1998 (received for review September 23, 1998)

ABSTRACT **Opitz syndrome (OS) is a genetically heterogeneous disorder characterized by defects of the ventral midline, including hypertelorism, cleft lip and palate, heart defects, and mental retardation. We recently identified the gene responsible for X-linked OS. The ubiquitously expressed gene product, *MID1*, is a member of the RING finger family. These proteins are characterized by an N-terminal tripartite protein–protein interaction domain and a conserved C terminus of unknown function. Unlike other RING finger proteins for which diverse cellular functions have been proposed, the function of *MID1* is as yet undefined. By using the green fluorescent protein as a tag, we show here that *MID1* is a microtubule-associated protein that influences microtubule dynamics in *MID1*-overexpressing cells. We confirm this observation by demonstrating a colocalization of *MID1* and tubulin in subcellular fractions and the association of endogenous *MID1* with microtubules after *in vitro* assembly. Furthermore, overexpressed *MID1* proteins harboring mutations described in OS patients lack the capability to associate with microtubules, forming cytoplasmic clumps instead. These data give an idea of the possible molecular pathomechanism underlying the OS phenotype.**

Opitz G/BBB syndrome (OS) is a congenital syndrome characterized by malformations involving several unrelated anatomical structures, all situated in the midline of the human body. Mental retardation associated with dysplasia of the corpus callosum, ocular hypertelorism (excessive distance between any paired organs, e. g. the eyes), cleft lip and cleft palate, laryngotracheo-esophageal fistulas, and genitourinary defects such as hypospadias are all prominent manifestations of the syndrome. Imperforate anus and hymen and cardiac abnormalities such as tetralogy of Fallot have also been described (1). By linkage analysis, two main gene loci, one on chromosome 22 and one on the X chromosome, were shown to be responsible for this heterogeneous disorder (2). Employing a positional cloning approach, we have recently identified a gene located at Xp22.3, designated *MID1*, and found that it is selectively mutated in patients suffering from Opitz syndrome (3).

The protein encoded by the *MID1* gene comprises four separate domains common to the RING finger proteins. Therefore, *MID1* represents a new member of this protein family. Three of the four conserved domains are part of an N-terminal tripartite motif consisting of the RING finger itself, a so-called B box (present in one or two copies), and an α-helical region capable of coiled-coil formation (4–6). Members of this protein family are involved in diverse cellular processes: *Xenopus* nuclear factor 7 (*XNF7*) was found to play an important role in dorsal/ventral patterning of the *Xenopus* embryo (7–9), whereas the promyelocytic protein (*PML*), the ret finger protein (*RFP-1*), and transcription intermediary factor (*TIF-1*) are protooncogenes (10–13). Furthermore, as some of the RING finger proteins are part of macromolecular complexes, the formation of which depends on an intact N terminus (11), the tripartite motif is thought to be involved in protein–protein interactions.

A second cluster of amino acids highly conserved between *MID1* and five other RING finger proteins (3) is located in the C terminus. The function of this protein domain is largely unknown except for the C terminus of murine butyrophilin, which was reported to be specifically associated with a 150-kDa cytoplasmatic protein (14). Surprisingly, all of the mutations identified in OS patients so far are located in the C terminus of the *MID1* protein (3, 15). This finding suggests that the C-terminal domain is critical for a functional *MID1* protein.

The cellular localization of RING finger proteins has been shown to be very important for their specific functions. In an attempt to shed light on the function of the *MID1* protein, we have studied its intracellular localization employing transfection of green fluorescent protein (GFP) fusion constructs into COS-7, MCF-7, and HeLa cells and into human fibroblasts. Unlike other RING finger proteins, *MID1* was not found in the nucleus but was confined to the cytoplasm. More detailed analysis revealed a close association of *MID1* with microtubules, whereas the introduction of mutations found in OS patients completely abolished microtubule association. Thus, our data establish a physiological role for *MID1* in microtubule dynamics. At the same time, they suggest a possible pathomechanism for OS.

MATERIALS AND METHODS

GFP Constructs and Site-Directed Mutagenesis. *GFP*-fusion constructs were generated by using the CLONTECH *GFP* system employing pGFP-N3 for the C-terminal and pEGFP-C1 for the N-terminal MID1 fusion. Inserts were amplified with Stratagene *Pfu* polymerase in the appropriate buffer containing 1 mM $MgCl_2$. Primers used for amplifying the complete translated region were GCTCAAGCTTCGATGGAAACAATGGAGTCAG and TCGAATTCTTCACGGCAGCTGCTCTGT for the N-terminal construct and GCT-

The publication costs of this article were defrayed in part by page charge payment. This article must therefore be hereby marked "*advertisement*" in accordance with 18 U.S.C. §1734 solely to indicate this fact.

PNAS is available online at www.pnas.org.

This paper was submitted directly (Track II) to the *Proceedings* office.

Abbreviations: OS, Opitz syndrome; GFP, green fluorescent protein.

†To whom reprint requests should be addressed at: Max-Planck Institute for Molecular Genetics, Ihnestrasse 73, 14195 Berlin, Germany. e-mail: schweiger@mpimg-berlin-dahlem.mpg.de.

CAAGCTTCGATGGAAACACTGGAGTCAG and TCGAATTCTCGGCAGCTGCTCTGTGCA for the C-terminal *MID1* construct. PCR products were digested with *Hin*dIII/*Eco*RI and subsequently isolated from low melting temperature agarose with the Qiagen (Chatsworth, CA) gel extraction kit.

Site-directed mutagenesis was performed by using the QuickChange kit from Stratagene. All oligonucleotides used were HPLC-purified.

Tissue Culture and Microtubule Stability Assay. COS-7 cells were purchased from the American Type Culture Collection and spread at 1×10^5 cells per well of a 6-well plate 1 day before transfection. Transfection was carried out following the CLONTECH protocol of the GFP system for liposome-mediated transfection by using Lipofectace (Gibco) at a ratio of 1.2:1 (liposome/vector). Expression was optimal 48 hours after transfection. For the microtubule stability assay, cells were incubated for 2 hours at increasing colcemid concentrations (range 50–400 ng/ml) and with 100 ng/ml of colcemid for 2–14 hours, respectively. The percentage of destroyed microtubules bundles was calculated by dividing the number of transfected cells with intact microtubules stained with indirect immunofluorescence by the total number of cells showing *GFP–MID1*-expression of one coverslip (350–500 cells counted per coverslip). This was done in three independent experiments.

MCF-7 cells, HeLa cells, and human fibroblasts were obtained from the Max-Planck Institute for Cell Biology (Ladenburg, Germany).

Family with OS and Mutation Analysis. A fibroblast cell line from an aborted fetus with OS was established from skin biopsy material and grown in Ham's F-10 (GIBCO and Sigma) nutrient medium with 20% fetal calf serum, 200 mM L-glutamine, penicillin, and streptomycin. Before abortion, the mother of the affected fetus had undergone prenatal diagnosis because her first son (SW) had presented with clinical signs of Opitz syndrome. Subsequent molecular analysis in our lab by SSCP (single strand conformation polymorphism; ref. 16) and sequencing revealed a 4-bp deletion in the C-terminal exon of MID1. The same mutation was found in the fetus, and autopsy thereby confirmed the diagnosis of OS.

Primers used for the amplification of the affected exon of *MID1* had the following sequences: ATGTGCAACATGGCTCATTG and GACACTTGTTCCACACGGTG.

Antibody Production. For antibody production for *MID1* detection, two peptides from the N terminus of *MID1*, GPNSPSETRRERAFD and LEHEDEKVNM, were synthesized, pooled, and used for rabbit immunization. After four boosts at 3-week intervals, high-titer serum was collected at 12 weeks post immunization. The antibody obtained was affinity-purified by chromatography on immobilized peptide CGNSPSETRRERAFD coupled to Sulfolink coupling gel (Pierce). Binding specificity was established via Western blots with protein expressed in *Escherichia coli* and in immunofluorescent experiments with *MID1*-overexpressing cells in the presence and absence of competing peptide. The antiserum recognized a single band migrating at 72 kDa, which was specifically suppressed by addition of antigenic peptide. The affinity-purified antibody was used with a titer of 1:25 for Western blots and 1:10 for immunofluorescence.

Immunofluorescence. Anti-tubulin antibodies were obtained from Serotec (MCA77S and MCA78S). For immunofluorescence, we used a modified standard protocol as described (17), with PBS buffer replaced by 1.2× PEM buffer (10× PEM contains 1M Pipes, 0.05M EGTA, and 0.02M $MgCl_2$, pH 7.0) to protect the microtubules. As a control, the anti-*MID1* antibody was preincubated with 100 μg/ml of each antigenic peptide for 30 minutes at room temperature.

Cell Fractionation and Immunoblot Analysis. Subcellular fractions of 1×10^7 primary embryonic fibroblasts were prepared as described (18) based on three differential centrifugation steps (1,000 × *g*, 17,500 × *g*, and 100,000 × *g*). Fractions were separated on a 7.5% SDS gel, transferred to nitrocellulose membranes, and subsequently incubated with an affinity-purified anti-*MID1* and two anti-tubulin antibodies (see above). Blots were incubated with horseradish peroxidase-conjugated anti-rabbit Fab fragments (Amersham Pharmacia) and developed with enhanced chemiluminescence reagents (Amersham Pharmacia) as specified by the manufacturer.

***In Vitro* Assembly of Microtubules.** HeLa microtubules were prepared from 4×10^7 cells according to a protocol described previously (19) by using Taxol to facilitate microtubule assembly. MID1/GFP-overexpressing COS-7 cells (1×10^6) were treated with 200 ng/ml colcemid overnight to destroy the microtubules, homogenized in 5 vol of microtubule assembly buffer (19), and centrifuged at 60,000 × *g* for 60 min. The supernatant was mixed with Taxol, GTP, and HeLa microtubules and incubated at 37°C for 30 min. The pellet of the subsequent ultracentrifugation of 30 min at 40,000 × *g* was washed once with Taxol-containing assembly buffer and analyzed by Western blot analysis. Membranes were probed sequentially with affinity-purified anti-*MID1* (see above) and anti-*GFP* purchased from CLONTECH. *In vitro* assembly of endogenous *MID1* protein was performed with cytosol of 1.7×10^7 primary embryonic fibroblasts prepared by using the same protocol as described above.

RESULTS

To study the intracellular localization of the *MID1* protein, we assembled two different *GFP-MID1* fusion constructs. Both constructs, an N-terminal *GFP* fusion and a C-terminal *GFP* fusion, were transfected into four different cell types, i. e. COS-7, MCF-7, and HeLa cells and primary human fibroblasts. Fluorescence microscopy revealed reticular cytoplasmic structures similar to cytoskeletal filaments in all cell types transfected with the C-terminal *GFP* fusion protein (Fig. 1*A*). Identical filamentous structures were observed on overexpression of native *MID1* protein in the same cell types and subsequent indirect immunfluorescence with a specific anti-*MID1* antibody (data not shown). The filaments could not be extracted with Triton X-100 up to a concentration of 1% (vol/vol). The nuclei were clearly devoid of filamentous structures and did not show any other fluorescent signal (Fig. 1*A*). Cells transfected with the N-terminal *GFP* construct showed diffuse cytoplasmic clumps (data not shown) which may be because of steric inhibitory effects of the *GFP* moiety on the C-terminal domain of *MID1* subsequently shown to be critical for cytoskeletal association (see below).

We next sought to define the cytoskeletal localization of *MID1* more precisely. Whereas association of *GFP-MID1* with actin fibers and intermediate filaments could be clearly excluded by using the corresponding antibodies (data not shown), indirect immunofluorescence with a mixture of two different rat anti-tubulin antibodies revealed a perfect colocalization of *GFP-MID1* with microtubules in COS-7, MCF-7, and HeLa cells and in primary human fibroblasts (Fig. 1*B*). The microtubules in *MID1*-transfected cells, in contrast to the microtubule pattern in wild-type cells, seem to be bundled by the overexpressed protein (Fig. 1 *A* and *B*).

In a separate set of experiments, endogenous *MID1* and tubulin were found to cofractionate in the same subcellular fractions (low-, medium-, and high-speed supernatants) of primary embryonic fibroblasts prepared by differential centrifugation (18), as detected by an affinity-purified anti-*MID1* antibody (Fig. 1*C*, *Upper*) and two anti-tubulin antibodies in a Western blot analysis (Fig. 1*C*, *Lower*). To further confirm the association of native endogenous *MID1* with microtubules, we reassembled microtubules purified from HeLa cells in the

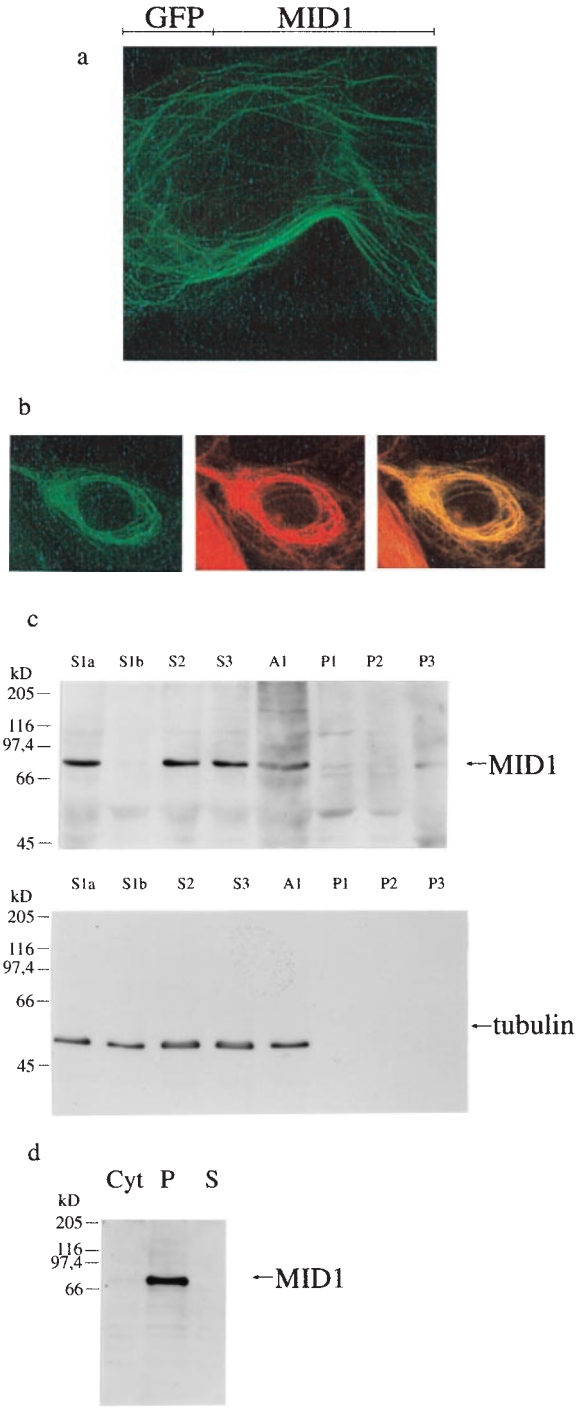

FIG. 1. Subcellular localization of *MID1*. (*a*) Filamentous structures revealed by transfection of COS-7 cells with the C-terminal *GFP-MID1* fusion protein. (*b*) Colocalization of the *GFP-MID1* fusion protein with microtubules in COS-7 cells. Overlap of the green fluorescent signal of *GFP-MID1* and the red staining of the anti-tubulin antibody yield yellow filaments, whereas the neighboring cell without *GFP-MID1* expression retains the red of the tubulin staining. (*c*) Western blot analysis of the subcellular fractions prepared from primary embryonic fibroblasts. *MID1* and tubulin are detected in the low- (S1a and S1b), medium- (S2), and high-speed supernatants (S3). The pellets (P1 low-speed pellet, P2 medium-speed pellet, and P3 high-speed pellet) contain neither *MID1* nor tubulin. A1 is an aliquot of the homogenized cells. Pellets were resuspended in 2 ml of detergent-containing buffer. Portions of each fraction (150 μl) were acetone-precipitated and resuspended in 40 μl of SDS loading buffer. On the blot incubated with a specific anti-*MID1* antibody (*Upper*), 20 μl of the resuspended acetone precipitates were loaded in each lane, on the blot incubated with anti-tubulin antibodies (*Lower*), 4 μl from a 1:10 dilution were loaded on each lane. Additional bands visible in the MID1 blot were caused by the high concentrations of protein loaded and were shown to be nonspecific by competition experiments with antigenic peptide (data not shown). (*d*) Western blot analysis of sedimented, reassembled HeLa microtubules in the presence of cytosol from primary embryonic fibroblasts. Each lane contains 20 μg of protein sample. Lane 1 contains an aliquot of the cytosol. The microtubule-containing pellet was loaded on lane 2. Lane 3 contains the supernatant after precipitation of the reassembled microtubules. A single band at 72 kDa is detected by incubation of the nitrocellulose blot with affinity-purified anti-MID1 in the microtubule-containing pellet and in the cytosol (very weak because of the low expression level of MID1).

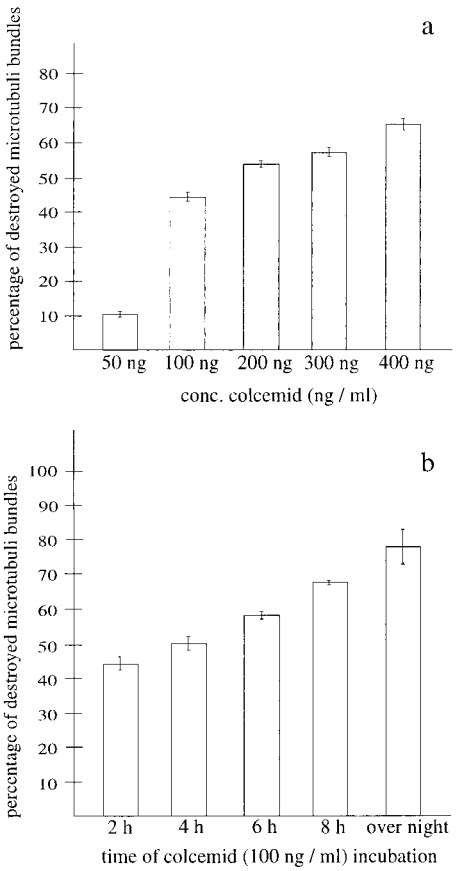

FIG. 2. GFP-MID1 fusion protein protects microtubules against depolymerizing agents like colcemid. (*a*) COS-7 cells transfected with GFP-MID1 were exposed to colcemid for 2 hours at the concentrations indicated. Data show represent mean ± SEM of three independent experiments. In each experiment, 350–500 transfected cells were visually scored for intact microtubule fibers (see *Materials and Methods*). (*b*) COS-7 cells were transfected with GFP-MID1 as in *a* and incubated with 100 ng/ml for the time periods indicated.

presence of cytosol derived from primary embryonic fibroblasts (19), followed by ultracentrifugation. The resulting microtubule-containing pellet was resuspended in SDS/PAGE buffer, and 20 μg of protein was analyzed by Western blotting. An aliquot of the supernatant and the cytosol containing the same amount of protein were loaded on the same gel. The *MID1*-specific affinity-purified antibody detected a single band of approximate 72 kDa, the size of endogenous *MID1*, in the pellet containing the microtubules, but not in the supernatant (Fig. 1*D*). The band detected in the cytosol was very weak because of the low expression level of endogenous MID1. Comparison of the cytosol and the microtubule-containing pellet demonstrate a specific enrichment of MID1 in the microtubule-containing pellet.

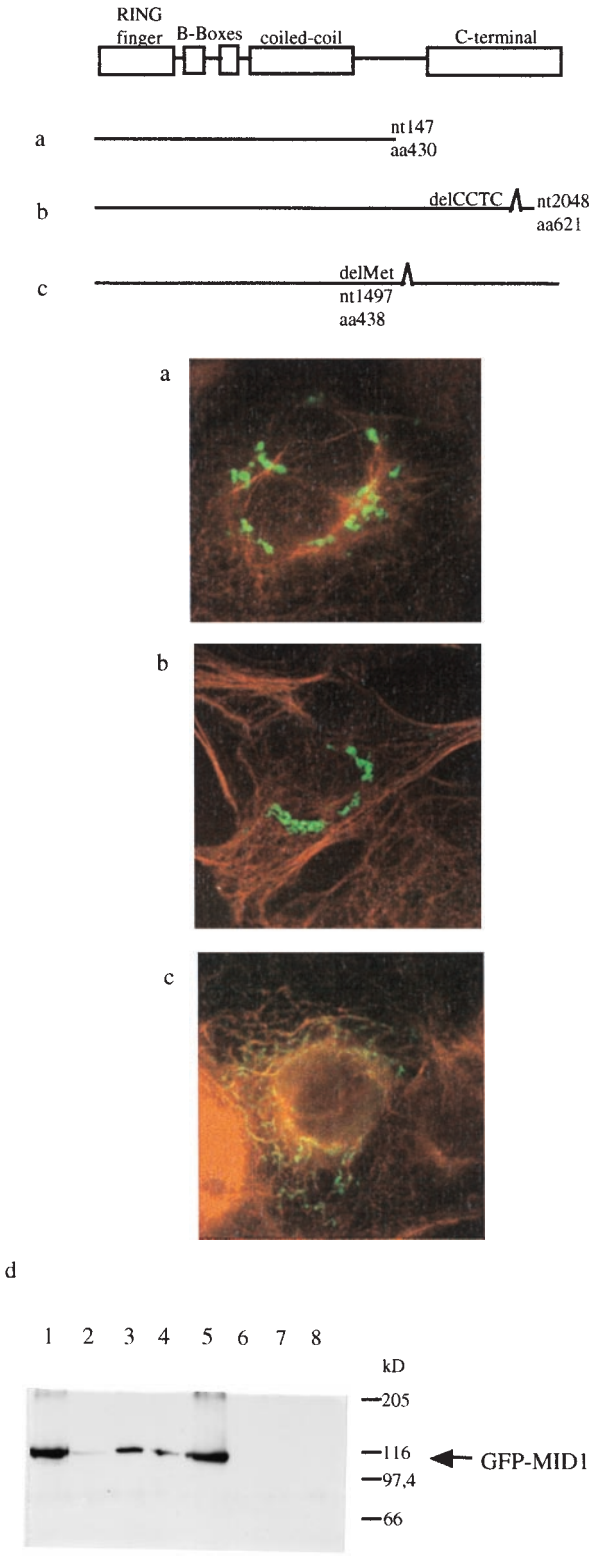

FIG. 3. Effects of mutations in the C terminus on the association of MID1 with microtubules. (*a*) COS-7 cells were transfected with a cDNA encoding a *GFP-MID1* fusion protein lacking the *MID1* C terminus. Microtubules were stained with anti-tubulin antibodies and a Cy3-labeled secondary antibody. (*b*) COS-7 cells were transfected with a GFP-MID1 fusion protein with a 4-bp deletion in the MID1 C terminus. This protein mutant was previously identified in family "W." Microtubules were stained with anti-tubulin antibodies and a Cy3-labeled secondary antibody. (*c*) Reduced microtubule association capacity of *GFP-MID1* lacking Met-438 of *MID1*, the MID1 mutant identified in family "OS5." Microtubules were stained with anti-tubulin antibodies and a Cy3-labeled secondary antibody. (*d*) Western blot of sedimented HeLa microtubules reassembled in the presence of cytosol of wild-type *GFP-MID1* (lanes 1–4) or mutated *GFP-MID1* (lanes 5–8), respectively. Each lane was loaded with 15 μg of protein of the microtubule-containing pellets (lanes 3 and 7), the same amounts of the respective cytosols (lanes 2 and 6), the acetone-precipitated supernatant left after microtubule reassembly (lanes 4 and 8); in lanes 1 and 5, 100 μg of the cell homogenates were loaded. A *GFP*-specific antibody detected protein of the expected size (100 kDa) only in the microtubule-containing pellet and the cytosol derived from the wild-type expressing cells (lanes 2 and 3), but not in the same fractions derived from the mutant-expressing cells (lanes 6 and7). A small amount also was detected in the acetone-precipitated supernatant from the experiments with the wild-type cells (lane 4). The homogenates (lanes 1 and 5) show that expression levels of GFP-MID1 was comparable in both experiments.

For further characterization of the microtubule bundles obtained in *GFP-MID1*-overexpressing cells, we incubated transfected COS-7 cells for 2 hours with increasing concentrations of colcemid, which is known to induce the depolymerization of microtubules. A concentration of 50 ng/ml, which destroys 100% of the microtubules in wild-type cells (ref. 20, and data not shown), did not affect microtubules in *GFP-MID1*-overexpressing cells. Higher concentrations of colcemid lowered the percentage of cells with intact microtubules, but even at concentrations as high as 400 ng/ml, eight times the concentration sufficient to destroy all microtubules in nonrecombinant cells, more than 30% of the microtubule bundles remained intact in the presence of *GFP-MID1* (Fig. 2*A*). Transfected COS-7 cells were also incubated for varying time periods ranging from 2 hours to overnight at a fixed colcemid concentration (100 ng/ml). Again, although an increasing duration of colcemid treatment did reduce the percentage of transfected cells with intact microtubules, even overnight incubation did not destroy all microtubule bundles in the overexpressing cells (Fig. 2*B*). Exposure to low temperatures also revealed a much higher stability of the microtubules in *GFP-MID1*-overexpressing cells compared with normal cells (data not shown). Overexpression of GFP alone did not cause any microtubule association under any of the conditions described (data not shown).

As all mutations found in OS patients are clustered near the C terminus of *MID1* (3, 15), we hypothesized that this part of the protein plays an important functional role. In this regard, it is of interest that we have identified the most C-terminally located mutation found to date, which is a 4-bp deletion starting at nucleotide 1,986 and resulting in a frameshift and a premature stop codon at nucleotide 2,048 that truncated the MID1 gene product by 47 aa. This mutation was found in a male infant with OS, his heterozygous mother, and in chorionic villus material obtained by biopsy at 11 weeks gestation in a subsequent pregnancy with a male fetus (Fig. 4).

To study the influence of the C terminus on the cellular localisation of *MID1* (Fig. 3), we designed three different constructs. One construct totally lacked the C terminus (Fig. 3*A*), whereas the others simulated gene products expressed in two OS patients. These two mutations were the 4-bp deletion at nucleotide 1,986 (amino acid 600) (Fig. 3*B*) described above and an in-frame 3-bp deletion leading to the loss of Met-438 (nucleotide 1,497) of *MID1* (3)(Fig. 3*C*). These mutations were introduced into the *GFP-MID1* plasmid by using site-directed mutagenesis. Truncation of the C terminus completely abolished the binding of the fusion protein to microtubules. Instead, the truncated protein formed clumps in the cytoplasm of the transfected cells (Fig. 3*A*). The same effect was observed with a construct carrying the 4-bp deletion (Fig. 3*B*), whereas the deletion of Met-438, although also causing clump formation, preserved some microtubule-binding activity of the fusion protein (Fig. 3*C*). For further confirmation of this finding, purified microtubules from HeLa cells were reassembled in the

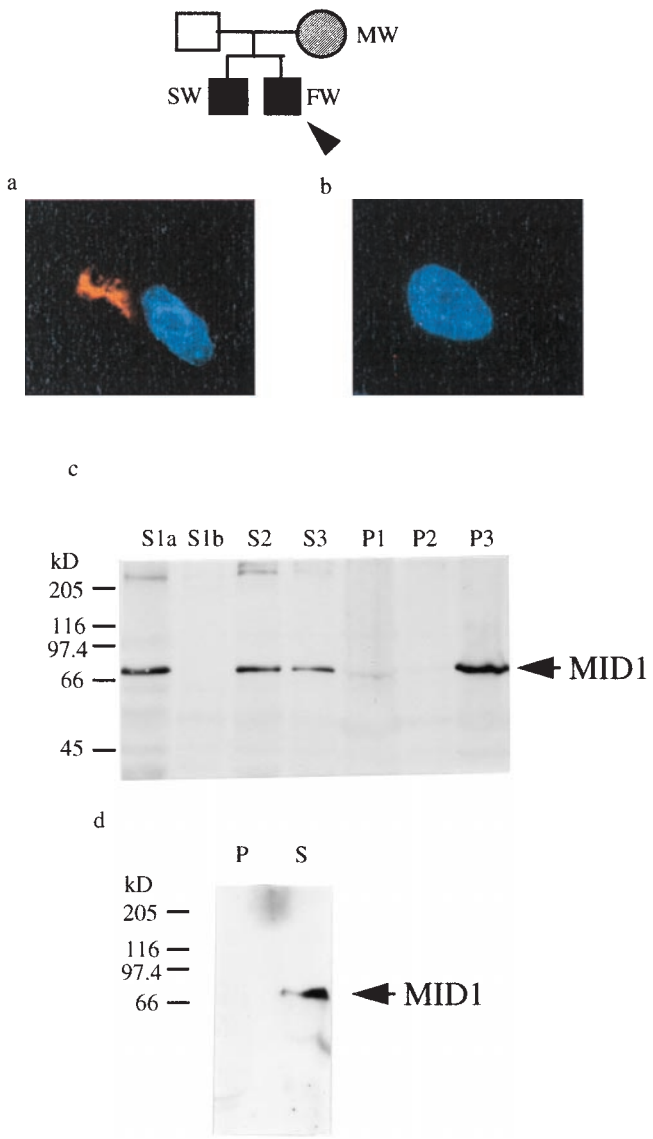

FIG. 4. Four-base pair deletion in a family with Opitz syndrome. (*a*) Immunofluorescence staining of fibroblasts from a fetus affected with Opitz syndrom (FW) with a *MID1*-specific antibody. Blue is the DAPI staining of the nuclei. Cytoplasmic clumps were detected with a Cy3-labeled secondary antibody. (*b*) Immunfluorescence with the same fibroblasts as in *A* carried out after preincubation of the anti-*MID1* antibody with antigenic N-terminal peptides. (*c*) Cell fractionation of embryonic fibroblasts from a fetus affected with Opitz syndrome. Pellets were resuspended in 2 ml of detergent-containing buffer as in Fig. 1*c*, and 150 μl of each fraction was separated on a 7.5% polyacrylamide gel, blotted, and probed with affinity-purified anti-MID1 antibody. In the lane of fraction S1a, the same amount of protein (100 μg) was loaded as was used for S1a in Fig. 1*c*. (*d*) Western blot analysis of sedimented, reassembled HeLa microtubules in the presence of cytosol of primary embryonic fibroblasts from an OS fetus; 20 μg of the microtubule-containing pellet (lane 1) and the acetone-precipitated, resuspended supernatant (lane 2) were loaded.

presence of cytosol from COS-7 cells transfected with either wild-type *GFP-MID1* or the *GFP-MID1* construct carrying the 4-bp deletion followed by ultracentrifugation (see *Materials and Methods*). Fifteen micrograms of the resulting pellets (Fig. 3*D*, lanes 3 and 7) and the same amounts of protein from the cytosols (Fig. 3*D*, lanes 2 and 6) from each experiment were analyzed by Western blot. In both fractions, a band of $\approx$100 kDa, the expected size of *GFP-MID1*, was detected with a specific anti-*GFP* antibody on expression of the wild-type *GFP-MID1*, but not of the *GFP-MID1* construct carrying the mutation (Fig. 3*D*). Comparison of the cytosol and the microtubule-containing pellet of the experiment carried out with the wild-type *GFP-MID1* again demonstrates a specific enrichment of *MID1* in the microtubule-containing pellet. In the case of the mutant, all protein is pelleted with the initial step of ultracentrifugation (data not shown), presumably because of the formation of cytoplasmic clumps. The supernatants of the two experiments were acetone-precipitated, resuspended in SDS/PAGE buffer, and loaded onto the same gel (Fig. 3*D*, lanes 4 and 8). A small portion of protein was found in the supernatant of the wild-type-expressing cells, but no protein was detected in the supernatant of the mutant-expressing cells. Cell homogenate protein (100 μg) from both experiments loaded onto the same gel shows similar expression levels of the wild-type and the mutant GFP/MID1 proteins (Fig. 3*D*, lanes 1 and 5).

The formation of cytoplasmic clumps was assigned to a defective *MID1* C terminus by studying the effect of several N-terminal mutations with a series of *GFP-MID1* constructs. In these studies we sequentially mutated the domains of the N-terminal motif, i.e., the RING finger, the two B boxes, and the coiled-coil domain. None of these mutations caused formation of cytoplasmic clumps. Instead, all of the resulting proteins associated with microtubules, although diffuse cytoplasmic background staining suggested a weakened binding (data not shown).

To clarify whether the formation of cytoplasmic clumps might indeed be relevant to the pathogenesis of OS, an embryonic fibroblast cell line was established from the aborted OS fetus (see above, Fig. 4). A *MID1*-specific, affinity-purified antibody was used in conjunction with a Cy3-labeled secondary antibody to analyze these fibroblasts by indirect immunofluorescence. In the cells of the OS fetus, cytoplasmic clumps of various sizes were detected (Fig. 4*A*), which were not found in the cytosol of a fibroblast cell line derived from a fetus of the same gestational age. Preincubation of the antibody with antigenic N-terminal peptides abolished the detection of cytoplasmic clumps (Fig. 4*B*), demonstrating the specificity of the signal. Our inability to detect filamentous structures in the control cell line may be because of the much lower focal concentration of the fluorescent signal finely distributed alongside the microtubules. In OS fibroblasts, the *MID1* protein might be visible because of a much better signal-to-noise ratio caused by the accumulation of the protein in the clumps.

Cell-fractionation experiments carried out with embryonic fibroblasts from the aborted OS fetus showed that a large fraction of the aberrant protein precipitated with the high-speed pellet P3 (Fig. 4*C*), indicating reduced solubility of the cytoplasmic clumps as compared with the native protein. In fibroblasts of the OS patient, the concentration of mutant MID1 protein was found to be similar to that of intact MID1 protein, as shown in Fig. 1*C*. Furthermore, a microtubule coassembly assay with extracts from OS fibroblasts revealed that the mutated MID1 protein that stays soluble after the initial ultracentrifugation step lacks microtubule-binding ability (Fig. 4*D*).

Last, comparison of microtubule stability to depolymerizing drugs such as colcemid and nocodazol in the OS embryonic fibroblasts and the age-matched control cell line did not reveal any significant difference (data not shown). This is not surprising, however, given that most cell types in OS patients, including fibroblasts, are apparently unaffected by a dysfunctional or nonfunctional *MID1* protein, due to as-yet-unidentified compensating mechanisms. Moreover, the microtubule stabilization property of *MID1* observed in overexpressing cells may also critically depend on expression levels. In this regard, it is of interest that murine MID1 was recently shown to be significantly higher expressed in ventral midline structures than in any other tissue (20).

DISCUSSION

The equilibrium of microtubule assembly and disassembly that influences essential cellular processes such as cell cycle, axonal outgrowth, and cellular migration (21) is tightly regulated by several microtubule-associated proteins. The filaments that result from transfecting a cDNA coding for a *GFP-MID1* fusion protein into several cell lines (Fig. 1) are strongly reminiscent of the bundled microtubules seen in cells transfected with *tau* or *MAP2* cDNAs (22–24), which are the most important regulators of microtubule dynamics in the nervous system. The loss of the microtubule-binding capability of *tau* protein has been shown to play a major role in the pathogenesis of Alzheimer's disease (25, 26). Similar to *MID1*, overexpressed *tau* stabilizes nascent bundles and has a protective effect against microtubule-depolymerizing agents such as colcemid (21). The protection of the *GFP-MID1*-covered microtubules against a cold stimulus was also similar to the effect reported for other microtubule-associated proteins (27).

A defective *MID1* gene product lacking its microtubule-stabilizing function would be assumed to have dramatic consequences for the cells affected. Still, mice homozygously deficient for MAP-type proteins display widely varying phenotypes ranging from almost no impairment seen in tau knock-out mice (28) to severe disorders in MAP1B knock-out mice which suffer from numerous neuronal abnormalities (29). Different MAPs may, at least in part, be able to substitute for each other, thus compensating for the loss of function of individual proteins. This may also hold for most tissues of OS patients, where noncompensated functional deficits are confined to special cells of the developing ventral midline. It also is possible that intact *MID1* function depends on the expression level. A recent paper describes significantly higher expression levels of *MID1* in cells that undergo mesenchyme–epithelium transformation, which is a characteristic process during ventral midline development (20). As it is impossible to obtain human cells from the developing ventral midline undergoing mesenchymal–epithelial transformation, a mouse model is of high importance for extended *in vivo* studies of the function of *MID1*.

All *MID1* mutations in OS patients reported to date affect the protein's C terminus (3, 15) (Fig. 4). Furthermore, we observed the formation of cytoplasmic clumps only in the presence of C-terminally mutated *MID1*, but not in the presence of N-terminal *MID1* mutants. Therefore, the clinical syndrome may involve an aberrant function of *MID1*, rather than simply its absence. Oligomerization with other proteins could exert a dominant negative effect by sequestering these proteins from their functional site. Alternatively, *MID1*-induced clumps may disturb microtubule homeostasis, analogous to the situation in Alzheimer's disease, where the abnormally expressed microtubule associated protein tau forms intracellular filamentous deposits leading to the degeneration of neuronal cells (25, 26, 30–32). Thus, it is conceivable that the clumps in the cytoplasm of OS patients mechanically interfere with cellular functions such as differentiation and cell movement. Actively migrating cells, such as those exiting the neural crest to shape the ventral midline, would be especially vulnerable to the detrimental effects of cytoplasmic clotting and/or microtubule dysregulation. A similar pathomechanism seems to play a role in lissencephaly, where the responsible gene product, Lis1, has also been shown to be highly involved in microtubule dynamics (33).

We thank "Family W." for their participitation and consent for publication. We thank Dr. Pippa Kyle for the prenatal procedures, Susann Freier, Ulrike Traub, and David Demege for tissue culturing, and Sabine Grüb for technical assistance. We thank Prof. Dr. M. Schweiger and Prof. Dr. Igor Dawid for critical discussion and Dr. D. Hirsch-Kauffmann Jokl for a thorough reading of the manuscript and helpful suggestions. The work was funded by the Deutsche Forschungsgemeinschaft (DFG) Grant RO389/17-2 (to H.H.R.).

1. Robin, N. H., Opitz, J. M. & Muenke, M. (1996) *Am. J. Med. Genet.* **62,** 305–317.
2. Robin, N., Feldman, L. J., Aronson, A. L., Mitchell, H., Weksberg, R., Leonard, C., Burton, B., Josephson, K., Laxóra, R., Aleck, V., *et al*. (1995) *Nat. Genet.* **11,** 459–461.
3. Quaderi, N. A., Schwerges, S., Laudenz, K., Franco, B., Rugarli, E., Berger, W., Feldman, G., Volta, M., Andolfi, G., Gilgenkrantz, S., *et al*. (1997) *Nat. Genet.* **17,** 285–291.
4. Reddy, B. A., Etkin, L. D. & Freemont, P. S. (1992) *Trends Biochem. Sci.* **17,** 344–345.
5. Freemont, P. S., Hanson, I. M. & Trowsdale, J. (1991) *Cell* **64,** 483–484 (lett.).
6. Freemont, P. S. *Ann. N.Y. Acad. Sci.* 174–192.
7. Li, X. & Etkin, L. D. (1993) *J. Cell Sci.* **105,** 389–395.
8. Li, X., Shou, W., Kloc, M., Reddy, B. A. & Etkin, L. D. (1994) *J. Cell Biol.* **124,** 7–17.
9. Gong, S.-G., Reddy, B. A. & Etkin, L. D. (1995) *Mech. Dev.* **52,** 305–318.
10. Weis, K., Ramboud, S., Lavau, C., Janson, J., Carvalho, T., Carmo-Fonseca, M., Lamond, A. & Dejean, A. (1994) *Cell* **76,** 345–356.
11. Dyck, J. A., Maul, G. G., Miller, W. H., Chen, J. D., Kakizuka, A. & Evans, R. M. (1994) *Cell* **76,** 333–343.
12. Isomura, T., Tamiya-Koizumi, K., Suzuki, M., Yoshida, S., Taniguchi, M., Matsuyama, M., Ishigaki, T., Sakuma, S. & Takahashi, M. (1992) *Nucleic Acids Res.* **20,** 5305–5310.
13. Le Douarin, B., Zedal, C., Gurnier, J. M., Lentz, Y., Tora, B., Henry, D., Gronemeyer, H., Chambor, P., & Losson, R. (1995) *EMBO J.* **14,** 2020–2033.
14. Ishii, T., Aoki, N., Noda, A., Adachi, T., Nakamura, R. & Matsuda, T. (1995) *Biochim. Biophys. Acta* **1245,** 285–292.
15. Gaudenz, K., Roessler, E., Quaderi, N., Franco, B., Feldman, G., Gasser, D. L., Wiltuer, B., Horzt, J., Martini, E., Opitz, J., *et. al*. (1998) *Am. J. Hum. Genet.* **63,** 703–710.
16. Orita, M., Iwahana, H., Kanazawa, H., Hayashi, K. & Sekiya, T. (1989) *Proc. Natl. Acad. Sci. USA* **86,** 2766–2770.
17. Sittler, A., Devys, D., Weber, C. & Mandel, J.-L. (1996) *Hum. Mol. Genet.* **5,** 95–102.
18. Gary, E. G. & Whittaker, V. P. (1962) *J. Anat.* **96,** 79–86.
19. Kimble, M., Khodjakov, A. L. & Kuriyama, R. (1992) *Proc. Natl. Acad. Sci. USA* **89,** 7693–7697.
20. Dalzotto, L., Quaderi, N., Elliott, R., Lingertelter, P., Carrel, L., Valsecchi, V., Montini, E., Yen, C., Chapman, V., Kalchera, I., *et al*. (1998) *Hum. Mol. Genet.* **7,** 489–499.
21. Hirokawa, N. (1994) *Curr. Opin. Cell Biol.* **6,** 74–81.
22. Barlow, S., Gonzalez-Garay, M. L., West, R. R., Olmsted, J. B. & Cabral, F. (1994) *J. Cell Biol.* **124,** 101–1029.
23. Gustke, N., Trinczek, B., Biernat, J., Mandelkow, E. M. & Mandelkow, E. (1994) *Biochemistry* **33,** 9511–9522.
24. Travis, G. H. (1991) *Nature (London)* **349,** 24.
25. Alonso, A. C., Grundke-Iqbal, I., Barra, H. S. & Iqbal, K. (1997) *Proc. Natl. Acad. Sci. USA* **94,** 298–303.
26. Alonso, A. C., Grundke-Iqbal, I. & Iqbal, K. (1996) *Nat. Med.* **2,** 783–787.
27. Harada, A., Oguchi, K., Okabe, S., Kuno, J., Terada, S., Ohshima, T., Sato-Yoshitake, R., Takei, Y., Noda, T. & Hirokawa, N. (1994) *Nature (London)* **369,** 488–491.
28. Edelmann, W., Zervas, M., Costello, P., Roback, L., Fischer, I., Hammarbach, J. A., Cowan, N., Davis, P., Wainer, B. & Kucherlapati, R. (1996) *Proc. Natl. Acad. Sci.* USA **93,** 1270–1275.
29. Hall, G. F., Yao, J. & Lee, G. (1997) *Proc. Natl. Acad. Sci.* **94,** 4733–4738.
30. Bosc, C., Cronk, J. D., Pirollet, F., Watterson, D. M., Haiech, J., Job, D. & Margolis, R. L. (1996) *Proc. Natl. Acad. Sci. USA* **93,** 2125–2130.
31. Goedert. M., Jakes, R., Spillantin, M. L., Klasegawa, M., Smith, M. J. & Crowther, R. A. (1996) *Nature (London)* **383,** 550–553.
32. Schweers, O., Mandelkow, E.-M., Biernat, J. & Mandelkow, E. (1995) *Proc. Natl. Acad. Sci.* USA **92,** 8463–8467.
33. Sapir, T., Elbaum, M. & Reiner, O. (1997) *EMBO J.* **16,** 6977–6984.